Journal of Flow Chemistry (2025) 15:137–143
https://doi.org/10.1007/s41981-025-00351-6

COMMUNICATIONS

Selective synthesis of phenylhydroxylamine under slug flow conditions using Bayesian optimization

Asami Yoshii[1] · Akira Fujii[1] · Yasuhiro Nishiyama[1] · Hajime Mori[1]

Received: 6 March 2025 / Accepted: 9 April 2025 / Published online: 22 April 2025

Abstract

Phenylhydroxylamine (PHA) derivatives are key chemical intermediates of nitrogen-containing organic compounds, however, their selective synthesis is challenging. Using Bayesian optimization, we attempted to streamline the reaction conditions for synthesizing PHAs in a microreactor to improve the yield of the target compound. Based on the results obtained in our previous work, the photoreduction of nitrobenzene was used for the selective synthesis of PHA under slug flow conditions. Furthermore, we examined the key factors responsible for the high synthetic selectivity. The optimization method helped us to optimize the experimental conditions required to achieve a yield of over 90% with only seven synthetic experiments. These results suggest that it is important to achieve a high reaction rate. Furthermore, additional experiments, cyclic voltammetry measurements, and calculations indicated that it is crucial to maintain the high redox potential of PHA under slug flow conditions with ethyl acetate. Finally, a batch reaction of the two phases was attempted to synthesize the target compound in comparison with the results of the flow reaction. Although the target compound was obtained in moderate yield with few byproducts, a prolonged reaction time was required. The flow reaction of the two phases slightly improved the synthesis selectivity and shortened the reaction time. We expect this reaction achieved by the merits of flow reactions to be useful for the synthesis of unstable PHAs.

Graphical Abstract

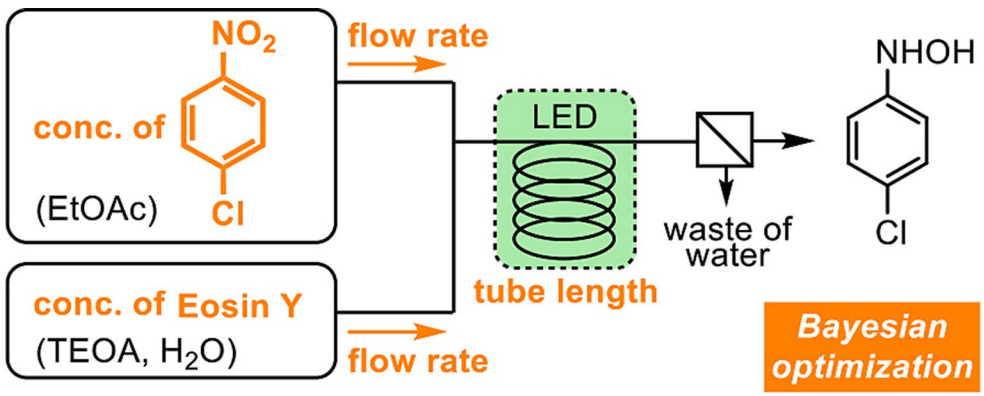

Keywords *N*-phenylhydroxylamine · Nitrobenzene photoreduction · Microreactor · Slug flow · Bayesian optimization

✉ Asami Yoshii
yoshii@wakayama-kg.jp

✉ Yasuhiro Nishiyama
y-west@wakayama-kg.jp

[1] Department of Chemical Engineering, Industrial Technology Center of Wakayama Prefecture, 60 Ogura, Wakayama 649-6261, Japan

Introduction

Phenylhydroxylamine (PHA) derivatives have attracted considerable attention because of their biological and pharmacological properties [1, 2] as well as their role as precursors for nitrogen-containing organic products [3–10]. Although

functionalization via PHAs has been recently explored [11–13], PHAs-intermediates in the synthesis of aniline via the reduction of nitrobenzene [14, 15], are unstable products. Their instability makes their synthesis laborious. A few reports describe selective synthetic methods to obtain PHAs from nitroarenes, including those using metal catalysts with hydrogen [16–19], metal catalysts with reducing agents [12, 20–24], Zn with ultrasound [25], and enzyme catalysts [26]. Therefore, alternative synthetic techniques are required.

Photoreactions are a key trend in organic synthesis; they offer clean and simple reaction methods because they proceed only by using photoirradiation instead of heating energy [27–37]. New methods have been reported for synthesizing PHAs via photoreactions. Photoreduction with methylhydrazine has been reported to reduce nitrobenzene to achieve selective PHAs in noncatalytic procedures [38]. However, the efficiency of photoreaction process is influenced by the length of the light path. Low photoreaction efficiency occurs in large reaction apparatuses with long path length, owing to the Beer–Lambert law. Using a flow reactor with a micrometer tube solves this challenge, as the short light path enables light irradiation of the entire solution [39].

Recently, we reported a new photoreduction method for producing PHA in a microreactor [40]. This method is based on previous reports describing the efficient photoreduction of nitrobenzene to azoxybenzene with high selectivity under flow conditions in a microreactor [41, 42]. The high efficiency and selectivity of the reaction are attributed to the short irradiation distance in the reactor and high mixing efficiency, achieved through flow reactions instead of batch-type photoreduction [43]. Furthermore, highly efficient production of azoxybenzene was achieved using slug flow with water/ethanol and fluorous solvents because of the high mixing and light confinement effect. In this process, induced photons are trapped in the segments containing the reactants due to the difference in the refractive index of each solvent [44, 45]. Hence, we attempted to perform slug flow with an organic solvent and water to synthesize the product with high efficiency thorough mixing and light confinement. In addition, we aimed to easily separate the products into organic solvents and the catalysts into water using a separator connected to the end of the flow reactor. Unexpectedly, this reaction under slug flow produced PHA as the main product.

Therefore, in this study, we optimized the reaction conditions for obtaining PHAs in a microreactor under slug flow to improve the yield of the target compound. Moreover, we elucidated the reason for synthesizing PHAs with high selectivity through additional experiments, measurements, and calculations. Furthermore, to optimize the appropriate reaction conditions, Bayesian optimization was applied in a few experiments, as it enables the prediction of subsequent experimental conditions [46, 47]. This optimization method is attractive because of its applicability [48–52] to synthesis in a flow reactor. Although there are a few examples of Bayesian optimization or machine-learning techniques in flow photoreactions [53, 54], we are not aware of any reports concerning the reduction of nitrobenzene.

Results and discussion

Utilization of bayesian optimization

First, we performed Bayesian optimization of this photoreduction using a slug-flow reaction. The synthesis of 4-chlorophenylhydroxylamine (**2**) from 4-chloro nitrobenzene (**1**) was carried out in two phases using water and ethyl acetate. The substrate, catalyst (Eosin Y), and triethanolamine were dissolved separately in each solvent (Fig. 1). Five experimental parameters were set: substrate concentration, Eosin Y concentration, the proportion of ethyl acetate to solvent, flow rate, and tube length. The program code previously reported by Fuse et al. was used to perform the Bayesian optimization [48]. Experimental parameters were input into a program code after setting the ratio and interval of each parameter, considering solubility, conditions for slug flow, and reaction time (Table 1). We used continuous discrete variables in the optimization campaign to ease the experimental preparation. The goal of this optimization was to achieve 90% yield of **2**. Using the prepared program, the computer outputted five initial reaction conditions with Latin hypercube sampling (LHS) [55] (Table 2, entries 1–5).

We then performed the experiments under the selected initial conditions and analyzed the crude material using ^{1}H NMR spectroscopy. The products obtained were **2**, **1**, 4,4′-*bis* (chloro) azoxybenzene (**3**) and 4-chloroaniline (**4**). Since the sum of the yields was less than 100%, other byproducts were generated, as indicated by various small peaks in the aromatic region. The initial five conditions yielded **2** in varying amounts (8–83%), with highest yield of 83% was obtained, (entry 3), and did not reach the desired yield (90%).

Next, Gaussian process regression (GPR) [56] was performed with the data obtained from the initial conditions to predict the next experimental conditions aimed at achieving a yield greater than 90% (Table 2, entries 6 and 7). Although the reaction performed under the conditions proposed by the first GPR, yielded **2** at 56%, the reaction proposed by GPR using data from entries 1–6 predicted a 97% yield. Only seven experiments were conducted to achieve the desired yield. Considering that five parameters needed to be optimized, this result demonstrated that previous optimization

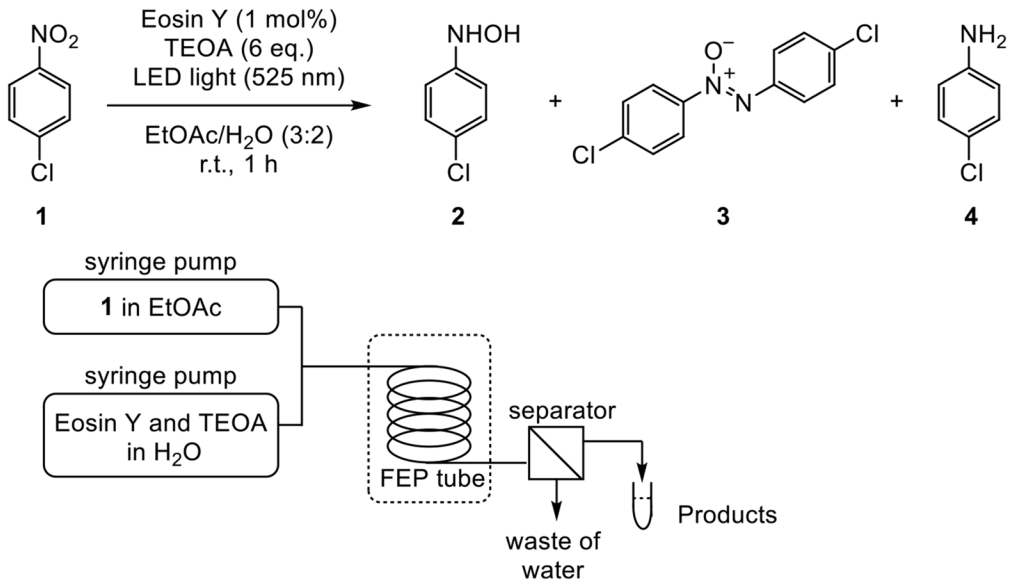

Fig. 1 Photoreduction of 4-chloro nitrobenzene (**1**) in flow microreactor

Table 1 The set range and interval of each parameter

conditions	range	interval	number
concentration of **1**	40–80 mM	10 mM	5
concentration of Eosin Y	0.40–16.00 mM	1.56 mM	11
proportion of ethyl acetate to solvent	0.2–0.9	0.1	8
flow rate	7.1–33.0 ml/h	0.2 ml/h	130
tube length	7/14/27 m	-	3

reached the target value extremely efficiently. Thus, Bayesian optimization facilitated the optimization of the photochemical synthetic conditions.

.

Necessary conditions for selective synthesis

Next, we attempted to elucidate why this reaction enables the selective production of PHA. The proposed reaction mechanism (Scheme 1) suggests that PHA was directly obtained from nitrosobenzene. Nitrosobenzene was reduced under the optimized conditions, led to the formation of PHA (Scheme S1). The key points for the selective synthesis of PHA are: (i) preventing the condensation of nitrosobenzene and PHA to form azoxybenzene and (ii) suppressing the further reduction of PHA to aniline. Firstly, we carefully examined the reaction conditions necessary to obtain the desired yield of **2** (Table 2, entry 7). The conditions were as follows: (1) the lowest concentration of **1**, (2) highest concentration of Eosin Y, and (3) lowest proportion of ethyl acetate. Thus, a high catalyst-to-substrate ratio is critical for increasing the reaction rate. Under these reaction conditions, nitrosobenzene was smoothly converted into PHA; effectively preventing condensation and the formation of azoxybenzene.

In addition, we examined the suppression of the further reduction of PHA. Since aniline was synthesized from nitrobenzene in ethanol and water in a previous study [43], we attempted to reduce **2** using fresh catalyst, but were unsuccessful (Scheme S2). These results indicated that the experimental conditions were not suitable for the reduction of PHA. We hypothesized that the key to suppressing further

Table 2 The selected initial conditions and the results

entry	conc. of **1** (mM)	conc. of Eosin Y (mM)	proportion of EtOAc to solvent	tube length (m)	flow rate (ml/h)	yield of **2** (%)[a]	recov. of **1** (%)[a]	yield of **3** (%)[a]	yield of **4** (%)[a]
1	60	3.52	0.9	27	9.7	8	66	2	2
2	40	9.76	0.2	14	25.1	56	1	4	4
3	50	14.44	0.3	7	22.5	83	0	2	2
4	80	0.40	0.6	27	29.9	15	77	0	0
5	70	9.76	0.5	14	13.5	64	0	28	4
6	80	14.44	0.7	7	7.1	56	16	4	2
7	40	14.44	0.2	7	32.9	96	0	3	1

[a]Determined by ^{1}H-NMR measurement using 1,3,5-trimethoxybenzene as an internal standard

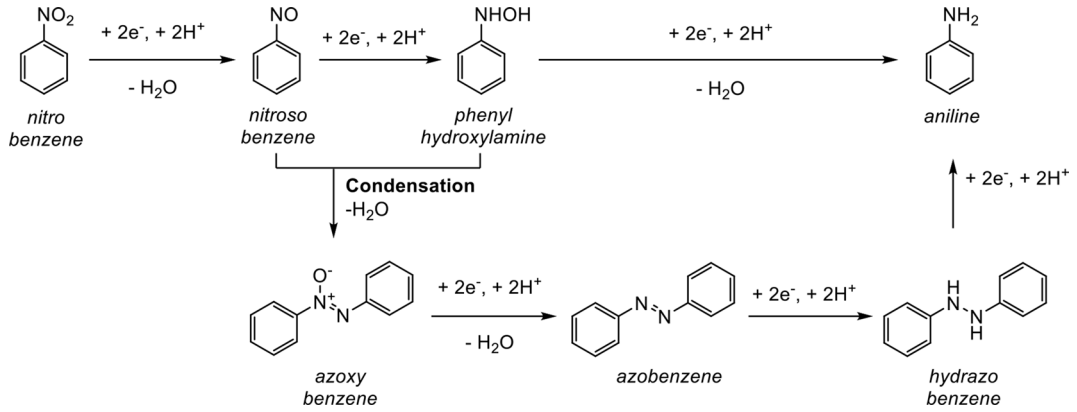

Scheme 1 Synthetic mechanism of aniline from nitrobenzene

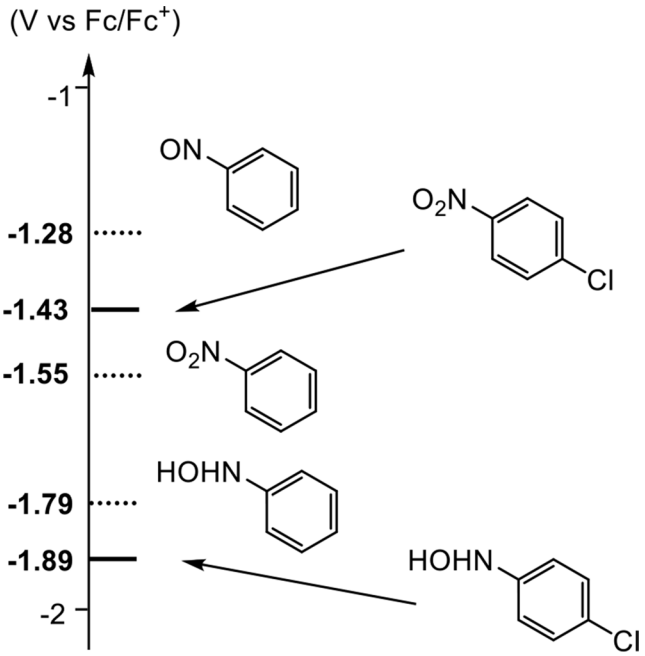

Fig. 2 Redox potentials ($E_{1/2}$) of each compound obtained by CV measurements in acetonitrile

reduction lies in the effect of the slug flow, consisting of water and ethyl acetate.

To verify our hypothesis, the cyclic voltammetry of each compound was first performed in acetonitrile, an organic solvent suitable for the measurement of the redox potentials (Fig. 2, Figure S1). Commercially available unsubstituted compounds were used for the comparison of the redox potentials. Although nitrobenzenes and nitrosobenzene have similar redox potentials, PHAs have higher redox potentials. This indicates that reducing PHA is more difficult than reducing nitrobenzene and nitrosobenzene. Further, DFT calculations with a polarizable continuum solvation model (PCM) [57] were conducted to examine the redox potential in ethyl acetate, water, and methanol. These solvents were selected because they were used in a previous study to selectively synthesize azoxybenzene [41]; and ethanol was selected as it is used to produce aniline in batch reactions [43] (Table S1). The PCM solvation model represents interactions between a PHA molecule and the solvent by placing the molecule in a solvent cavity with a specific dielectric constant [58]. Generally, redox potentials are estimated based on the lowest unoccupied molecular orbital (LUMO) levels [59]; thus, we checked the LUMO levels of PHA in each solvent set using the PCM model. The calculated results show that PHA has higher LUMO levels in ethyl acetate than in water, methanol, or ethanol, implying that the reduction of PHA is more difficult in ethyl acetate as compared to other solvents. In addition, because the catalyst and substrate were separated by the two-phase solution, electron transfer from Eosin Y to PHA at the solution interface was expected to be slow [60, 61]. Based on these results, the suppression of condensation and further reduction through this reaction method resulted in highly selective synthesis of PHA.

Comparison with batch reaction

To confirm the advantages of the flow reactor, a comparison was made between the flow reactor and batch reactor. Glass flasks were used as batch reactors, and the experiment was conducted under the optimal conditions used in the flow reactor (Scheme 2). The target compound was obtained in 89% yield with 5% azoxybenzene and 5% aniline as byproducts. Considering that the product was synthesized with a 96% yield in the flow reactor, the synthetic selectivity in the batch reactor was slightly lower than that in the flow reactor. Additionally, we compared the productivity of flow and batch reactors. The production rate in the flow reactor was 36.7 mg/h, whereas in the batch reactor it was 16.9 mg/h. This indicates that the reaction rate in the batch reactor was slower than that in the flow reactor, with a high slug flow mixing efficiency.

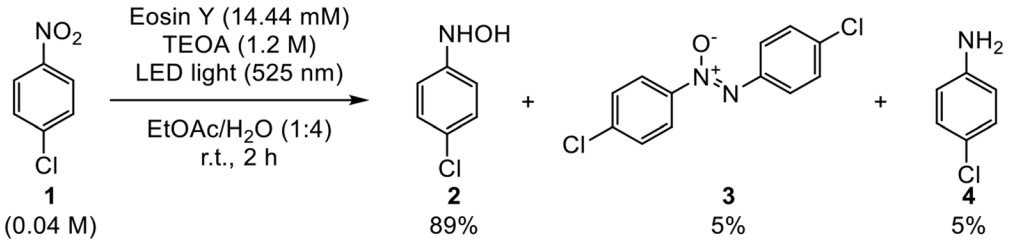

Scheme 2 Batch reaction in glass flasks with optimized reaction conditions

Conclusion

In this study, we investigated the synthesis of PHA from nitrobenzene using a flow microreactor with a slug flow of an organic solution and water. Bayesian optimization, enabled to achieve the highest yield of 96% after seven optimization steps. Additional experiments, measurements, and calculations revealed that the key to the high selectivity of PHA lies in the suppression of condensation and further reduction of the target compound. These results were accomplished by controlling both the reaction rate and reduction energies. Thus, our photoreaction method is effective for the synthesis of unstable PHAs.

Experimental

General information

Spectrograde solvents (EtOAc and water) were used throughout the work. All commercially available reagents were used without further purification. Particularly, 1,3,5-trimethoxybenzene as an internal standard was purchased with the qNMR grade. ^{1}H nuclear magnetic resonance (NMR) and ^{13}C NMR spectra were recorded at 400 and 100 MHz (Bruker Co. Ltd. Avance 400 and III 400 HD), respectively, and chemical shifts were represented as δ-values relative to internal standard TMS. Abbreviation is as follow: dd (double doublet). LC-MS measurement was recorded by Waters Co. Xevo G2-XS QTof. CV measurements were recorded using HOKUTO DENKO Co. HZ-7000. All DFT calculations were performed by B3LYP with the 6-31G(d, p) basis set employing the PCM solvation model, using Gaussian 16 program.

Photoreaction set-up

FEP tube (internal diameter (ID) = 1 mm) was used as a microreactor. The path length of tube is 1 mm. Tape-type green LED (5050type 60 LED/m Non-waterproof, consumed electric power 6 W/m) was utilized as the light source. Three different lengths of tape-type LED were made to match the length of the tube (4.4 m (261 tips) for 7 and 14 m tubes; 5.1 m (307 tips) for 27 m tubes). The way of photoirradiation is the same as our previous paper [41]. Reaction mixture was separated by a separator (Zaiput Flow Technologies Co. SEP-10) set at output of microreactor.

Synthetic methods (General)

Procedure for the photoreduction of 4-chloronitrobenzene as follows: 4-Chloronitrobenzene was dissolved in organic solvent degassed by Ar gas. Then, appropriate equivalents of triethanolamine and Eosin Y (tetrabromofluorescein) were added in water and degassed by Ar gas. The pH value of water solution was adjusted to 8.5 by adding concentrated HCl aqueous solution, because this pH value is the best condition for this photoreaction proceeding [43]. After adjusting the pH, each solution was pull out by using gas-tight syringes and syringe pumps controlled by appropriated flow rate, and mixed with a T-shape mixer to make slug flow. The mixed solution with slug flow was irradiated by the LED light for photoreduction. After photoreaction, the solution was separated to organic phase and water phase by the separator, and organic phase was collected. The concentration of the collected solution is adjusted by using a rotary evaporator, by adding 1,3,5-trimethoxybenzene, and measured ^{1}H-NMR. For isolation of a target PHA, collected organic phase was washed with saturated $NaHCO_3$ aqueous solution (15 mL) and saturated NaCl solution (15 mL), dried over anhydrous Na_2SO_4.

4-Chlorophenylhydroxylamine (2) [20, 38]: ^{1}H-NMR (400 MHz, $CDCl_3$): δ = 7.24 (2 H, dd), 6.93 (2 H, dd) ppm; ^{13}C-NMR (100 MHz, $CDCl_3$): δ = 148.20, 128.93, 127.17, 115.82 ppm; HRMS (LC-MS) *m/z* $[M+H]^+$ calcd for $C_6H_7ClNO^+$ 144.0211, found 144.0212.

Synthetic methods of batch reaction (shown in Scheme 2)

4-Chloronitrobenzene (41.8 mg, 0.265 mmol) was dissolved in ethyl acetate (6.6 mL) degassed by Ar gas. Then, triethanolamine (5.94 g, 39.8 mmol) and Eosin Y (308 mg, 0.475 mmol) were added in water (33 mL) degassed by Ar gas. The pH value of water solutions was adjusted to 8.5 by

adding concentrated HCl aqueous solutions. After adjusting the pH, each solution was put into a glass shrink (internal diameter (ID) = 22 mm), and mixed with a magnetic starring bar vigorously. The mixed solution was irradiated by the LED light for photoreduction until confirmed that the starting material was disappeared by reaction tracking of ^{1}H-NMR measurement. After photoreaction, the solution was separated to organic phase and water phase, and organic phase was collected. The concentration of the collected solution is adjusted by using a rotary evaporator, by adding 1,3,5-trimethoxybenzene, and measured ^{1}H-NMR to obtain NMR yields.

Optimization algorithm

Bayesian optimization was performed using the same the program code reported by Sugisawa N et al. [48] with a default arbitrary parameter to produce Gaussian Processes (GP) model. We used Latin hypercube sample (LHS) to select 5 initial experiments and the upper confidence bound (UCB) acquisition function with a default arbitrary parameter to identify subsequent reaction conditions with GP model.

Supplementary Information The online version contains supplementary material available at https://doi.org/10.1007/s41981-025-00351-6.

Acknowledgements We would like to thank Editage (www.editage.jp) for English language editing.

Declarations

Competing interests The authors declare that they have no known conflicts of interest/competing interests.

References

1. Gross P, Smith RP (1985) Biologic activity of Hydroxylamine: A review. Crit Rev Toxicol 14:87–99
2. Clark KB, Wayner DDM (1996) Are relative bond energies a measure of radical stabilization energies? J Am Chem Soc 118:8777–8781
3. Abbayes HD, Alper H (1977) Phase-transfer catalyzed and two-phase reactions of aromatic nitro compounds with iron carbonyls. J Am Chem Soc 99:98–101
4. Alper H, Amaratunga S (1980) The ruthenium carbonyl catalyzed reduction of nitro compounds by phase transfer catalysis. Tetrahedron Lett 21:2603–2604
5. Oro' J, Fritz KR, Master F (1959) Amino acid synthesis from formaldehyde and hydroxylamine. Arch Biochem Biophys 85:115–130
6. Becker AR, Sternson LA (1980) General catalyzed condensation of nitrosobenzene and Phenylhydroxylamine in aqueous solution. J Org Chem 45:1708–1710
7. Goti A, Sarlo FD, Romani M (1994) Highly efficient and mild synthesis of nitrones by catalytic oxidation of hydroxylamines with tetra-*n*-propylammonium perruthenate. Tetrahedron Lett 35:6571–6574
8. Kato T, Tabei K, Kawashima E (1976) Studies on ketene and its derivatives. LXXXII. Reaction of diketene with *N*-Phenylhydroxylamine derivatives. Chem Pharm Bull 24:1544–1551
9. Keilin D, Hartree EF (1943) Reactions of Hæmoglobin and its derivatives with phenyl hydroxylamine and nitrosobenzene. Nature 151:390–391
10. Salehzadeh H, Mashhadizadeh MH (2019) Nitrone synthesis via pair electrochemical coupling of Nitro-Compounds with benzyl alcohol derivatives. J Org Chem 84:9307–9312
11. Xi Z, Liu XJ, Guo Z, Gao Z, Yu ZX, Gao H (2023) Regioselective Umpolung para-C–H functionalization of arylhydroxylamines. Nat Synthesis 2:778–788
12. Hojczyk KN, Geng P, Zhan C, Ngai MY (2014) Trifluoromethoxylation of Arenes: synthesis of ortho-Trifluoromethoxylated aniline derivatives by OCF_3 migration. Angew Chem Int Ed 53:14559–14563
13. Ichikawa S, Zhu S, Buchwald SL (2018) A modified system for the synthesis of enantioenriched *N*-Arylamines through Copper-Catalyzed hydroamination. Angew Chem Inter Edi 57:8714–8718
14. Haber F (1898) Gradual electrolytic reduction of nitrobenzene with limited cathode potential. Z Elektrochem Angew Phys Chem 22:506–514
15. Blaser HU (2006) A golden boost to an old reaction. Science 313:312–313
16. Takenaka Y, Kiyosu T, Choi JC, Sakakura T, Yasuda H (2009) Selective synthesis of N-aryl hydroxylamines by the hydrogenation of nitroaromatics using supported platinum catalysts. Green Chem 11:1385–1390
17. Chen G, Xu C, Huang X, Ye J, Gu L, Li G, Tang Z, Wu B, Yang H, Zhao Z, Zhou Z, Gu G, Zheng N (2016) Interfacial electronic effects control the reaction selectivity of platinum catalysts. Nat Mater 15:564–569
18. Karwa SL, Rajadhyaksha RA (1987) Selective catalytic hydrogenation of nitrobenzene to Phenylhydroxylamine. Ind Eng Chem Res 26:1746–1750
19. Chen J, Lin X, Xu F, Chai K, Ren M, Yu X, Su W, Liu F (2023) An efficient continuous flow synthesis for the Preparation of N-Arylhydroxylamines: via a DMAP-Mediated hydrogenation process. Molecules 28:2968–2984
20. Jawale DV, Gravel E, Boudet C, Shah N, Geertsen V, Li H, Namboothiri INN, Doris E (2015) Selective conversion of nitroarenes using a carbon nanotube–ruthenium nanohybrid. Chem Commun 51:1739–1742
21. Shil AK, Das P (2013) Solid supported platinum(0) nanoparticles catalyzed chemo-selective reduction of nitroarenes to N-arylhydroxylamines. Green Chem 15:3421–3428
22. Ren P, Dong T, Wu S (1997) Synthesis of N-Arylhydroxylamines by Antimony-Catalyzed reduction of nitroarenes. Synth Commun 27:1547–1552
23. Doherty S, Knight JG, Backhouse T, Summers RJ, Abood E, Simpson W, Paget W, Bourne RA, Chamberlain TW, Stones R, Lovelock KRJ, Seymour JM, Isaacs MA, Hardacre C, Daly H, Rees NH (2019) Highly selective and Solvent-Dependent reduction of nitrobenzene to N-Phenylhydroxylamine, azoxybenzene, and aniline catalyzed by Phosphino-Modified polymer immobilized ionic Liquid-Stabilized AuNPs. ACS Catal 9:4777–4791
24. Pu X, Zhang B, Su Y (2019) Heterogeneous photocatalysis in microreactors for efficient reduction of nitrobenzene to aniline: mechanisms and energy efficiency. Chem Eng Technol 42:2146–2153
25. Liu S, Wang Y, Yang X, Jing J (2012) Selective reduction of nitroarenes to *N*-arylhydroxylamines by use of Zn in a CO_2–H_2O system, promoted by ultrasound. Res Chem Inter 38:2471–2478

26. Yanto Y, Hall M, Bommarius AS (2010) Nitroreductase from Salmonella typhimurium: characterization and catalytic activity. Org Biomol Chem 8:1826–1832
27. Yu XY, Chen JR, Xiao WJ (2021) Visible Light-Driven Radical-Mediated C–C bond cleavage/functionalization in organic synthesis. Chem Rev 121:506–561
28. Srivastava V, Singh PK, Srivastava A, Singh PP (2020) Recent application of visible-light induced radicals in C–S bond formation. RSC Adv 10:20046–20056
29. Zhou WJ, Wu XD, Miao M, Wang ZH, Chen L, Shan SY, Cao GM, Yu DG (2020) Light runs across Iron catalysts in organic transformations. Chem Eur J 26:15052–15064
30. Barata-Vallejo S, Postigo A (2020) New Visible-Light-Triggered photocatalytic trifluoromethylation reactions of Carbon–Carbon multiple bonds and (Hetero)Aromatic compounds. Chem Eur J 26:11065–11084
31. Zhou QQ, Zou YQ, Lu LQ, Xiao WJ (2019) Visible-Light-Induced organic photochemical reactions through Energy-Transfer pathways. Angew Chem Int Ed 58:1586–1604
32. Chuentragool P, Kurandina D, Gevorgyan V (2019) Catalysis with palladium complexes photoexcited by visible light. Angew Chem Int Ed 58:11586–11598
33. Huang C, Li XB, Tung CH, Wu LZ (2018) Photocatalysis with quantum Dots and visible light for effective organic synthesis. Chem Eur J 24:11530–11534
34. Marzo L, Pagire SK, Reiser O, König B (2018) Visible-Light photocatalysis: does it make a difference in organic synthesis?? Angew Chem Int Ed 57:10034–10072
35. Lang X, Chen X, Zhao J (2014) Heterogeneous visible light photocatalysis for selective organic transformations. Chem Soc Rev 43:473–486
36. Zou YQ, Chen JR, Xiao WJ (2013) Homogeneous Visible-Light photoredox catalysis. Angew Chem Int Ed 52:11701–11703
37. Prier CK, Rankic DA, MacMillan DWC (2013) Visible light photoredox catalysis with transition metal complexes: applications in organic synthesis. Chem Rev 113:5322–5363
38. Kallitsakis MG, Ioannou DI, Terzidis MA, Kostakis GE, Lykakis IN (2020) Selective photoinduced reduction of nitroarenes to N-Arylhydroxylamines. Org Lett 22:4339–4343
39. Su Y, Straathof NJW, Hassel V, Noël T (2014) Photochemical transformations accelerated in Continuous-Flow reactors: basic concepts and applications. Chem Eur J 20:10562–10589
40. Fujii A, Nishiyama Y, Yoshii A, Mori H (2023) Selective photoreduction of nitrobenzenes using microreactor. Chem TIMES 4:27–31
41. Nishiyama Y, Fujii A, Mori H (2019) Selective synthesis of azoxybenzenes from nitrobenzenes by visible light irradiation under continuous flow conditions. React Chem Eng 4:2055–2059
42. Nishiyama Y, Fujii A, Mori H (2022) Photoreduction synthesis of various azoxybenzenes by visible-light irradiation under continuous flow conditions. J Flow Chem 12:71–77
43. Yang XJ, Chen B, Zheng LQ, Wu LZ, Tung CH (2014) Highly efficient and selective photocatalytic hydrogenation of functionalized nitrobenzenes. Green Chem 16:1082–1086
44. Nakano M, Nishiyama Y, Tanimoto H, Morimoto T, Kakiuchi K (2016) Remarkable improvement of organic photoreaction efficiency in the flow microreactor by the slug flow condition using water. Org Process Res Dev 20:1626–1632
45. Nakano M, Morimoto T, Noguchi J, Tanimoto H, Mori H, Tokumoto S, Koishi H, Nishiyama Y, Kakiuchi K (2019) Accelerated organic photoreactions in flow microreactors under gas-Liquid slug flow conditions using N_2 gas as an unreactive substance. Bull Chem Soc Jpn 92:1467–1473
46. Shields BJ, Stevens J, Li J, Parasram M, Damani F, Alcarado JIM, Janey JM, Adams RP, Doyle AG (2021) Bayesian reaction optimization as a tool for chemical synthesis. Nature 590:89–96
47. Burger B, Maffettone PM, Gusev VV, Aitchison CM, Bai Y, Wang X, Li X, Alston BM, Li B, Clowes R, Rankin N, Harris B, Spick RS, Cooper AI (2020) A mobile robotic chemist. Nature 583:237–241
48. Sugisawa N, Sugisawa H, Otake Y, Krens RV, Nakamura H, Fuse S (2021) Rapid and mild One-Flow synthetic approach to unsymmetrical sulfamides guided by bayesian optimization. Chem Methods 1:484–490
49. Kondo M, Sugizaki A, Khalid MI, Wathsala HDP, Ishikawa K, Hara S, Takaai T, Washio T, Takizawa S, Sasai H (2021) Energy-, time-, and labor-saving synthesis of α-ketiminophosphonates: machine-learning-assisted simultaneous multiparameter screening for electrochemical oxidation. Green Chem 23:5825–5831
50. Ashikari Y, Tamaki T, Takahashi Y, Yao Y, Atobe M, Nagaki A (2022) Investigation of parameter control for electrocatalytic semihydrogenation in a Proton-Exchange membrane reactor utilizing bayesian optimization. Front Chem Eng 3:819752–819752
51. Nambiar AM, Breen CP, Hart T, Kulesza T, Jamizon TF, Jensen KF (2022) Bayesian optimization of Computer-Proposed multistep synthetic routes on an automated robotic flow platform. ACS Cent Sci 8:825–836
52. Liang R, Duan X, Zhang J, Yuan Z (2022) Bayesian based reaction optimization for complex continuous gas–liquid–solid reactions. React Chem Eng 7:590–598
53. Slattery A, Wen Z, Tenblad P, Sanjosé-Orduna J, Pintossi D, Den Hartog T, Noël T (2024) Automated self-optimization, intensification, and scale-up of photocatalysis in flow. Science 383. https://doi.org/10.1126/science.adj181
54. Buglioni L, Raymenants F, Slattery A, Zondag DA, Noël T (2022) Technological innovations in photochemistry for organic synthesis: flow chemistry, High-Throughput experimentation, Scale-up, and photoelectrochemistry. Chem Rev 122:2752–2906
55. Kondo M, Wathsala HDP, Ishikawa K, Yamashita D, Miyazaki T, Ohno Y, Sasai H, Washio T, Takizawa S (2023) Bayesian Optimization-Assisted screening to identify improved reaction conditions for Spiro-Dithiolane synthesis. Molecules 28:5180–5180
56. Rasmussen CE, Williams CKI (2006) Gaussian processes for machine learning. MIT Press
57. Cancès E, Mannucci B, Tomasi J (1997) A new integral equation formalism for the polarizable continuum model:theoretical background and applications to isotropic and anisotropic dielectrics. J Chem Phys 107:3032–3041
58. Wang H, Emanuelsson E, Banerjee A, Ahuja R, Strømme M, Sjödin M (2020) Effect of cycling ion and solvent on the redox chemistry of substituted Quinones and solvent-Induced breakdown of the correlation between redox potential and Electron-Withdrawing power of substituents. J Phys Chem C 124:13609–13617
59. Conradie J (2015) A frontier orbital energy approach to redox potentials. J Phys: Conf Ser 633:012045
60. Starks CM (1971) Phase-transfer catalysis. I. Heterogeneous reactions involving anion transfer by quaternary ammonium and phosphonium salts. J Am Chem Soc 93:195–199
61. Cheng Y, Schiffrin DJ (1993) A.C. Impedance study of rate constants for two-phase electron-transfer reactions. J Chem Soc Faraday Trans 89:199–205